

# Investigation of magnetic field by the Hall sensors embedded into magnetic bearing poles

Adam Krzysztof PIŁAT, Rafał BIESZCZAD, Hubert MILANOWSKI

*AGH University of Science and Technology  
Faculty of Electrical Engineering, Automatics, Computer Science and Biomedical Engineering  
Department of Automatic Control and Robotics  
Al. A. Mickiewicza 30, 30-059 Krakow, POLAND  
ap@agh.edu.pl, rafbiesz@agh.edu.pl, milan@agh.edu.pl*

## Abstract

A typical eight poles heteropolar active radial magnetic bearing configuration, consisting of Hall sensors embedded in the poles, is a research target. The active magnetic bearing operates without a safety bearing, and therefore identification was carried out in the maximum range of rotor displacement. The magnetic field was investigated experimentally using digital twin simulations developed in COMSOL Multiphysics software. The conducted research showed nonlinear dependencies of the magnetic flux density measured in the pole pieces as a function of the current, position, and orientation of the rotor. Typically used formulas that describe the relationships between force, magnetic flux density, current, and distance have been shown so that they are not to be used for arbitrary bearing configurations, rotor positions, and orientations due to simplifying assumptions.

**Keywords:** active magnetic bearing, Hall sensor, nonlinearity, identification, digital twin

## 1. Introduction

The heteropolar configuration of an active radial magnetic bearing (AMB), comprising eight pole pieces, has emerged as a widely adopted solution for numerous devices. Despite its common utilisation, this configuration remains an active area of research that encompasses both dynamic modelling and control aspects. A different class of control methodologies, known as the flux-based control algorithm, emerges as a viable approach to achieve enhanced positioning precision. Direct flux control requires real-time acquisition of air gap flux density information, which can be accomplished through observer-based techniques or direct measurements. To determine the air-gap flux density in AMBs, Hall sensors must be positioned within the air-gap. However, due to nominal air gap distances of 500  $\mu\text{m}$  or less, it is necessary to use ultrathin sensors or embed them in slots manufactured in the pole surface. Recent research has produced promising results in the development of thin Bismuth Hall sensors Ernst et al. (2016, 2020). Another research avenue pursued involves the fabrication of Hall sensors using a highly thin flexible Kapton foil Mystkowski et al. (2019). An economically viable approach involves the use of standard Hall sensors, which are mounted within slots manufactured on the surface of the pole Voigt & Santos (2012). By embedding the Hall sensors, their fragility is protected, albeit at the expense of a slight decrease in the effective pole area. Consequently, the maximum force achievable from AMBs is reduced by 2%, which might be negligible Kjølhede & Santos (2006), Voigt et al. (2017).

In Chowdhury & Sarjaš (2016) an unscented Kalman filter was used to estimate the position of the levitating body with a permanent magnet attached. UKF is designed based on nonlinear model derived with the Finite Element Method. The filter input is a measurement from the Hall sensor installed directly on the electromagnet surface. The estimated position was utilised as a feedback for nonlinear controller obtained on the basis of back-stepping technique and for a classic linear PID. In Miguel et al. (2018) the position of a levitating ferromagnetic ball is obtained using the measurement of the Hall sensor and the current sensor based on the dependency between the 3 signals identified numerically.

The concept of control based on the Hall sensor embedded in the stator pole was selected by Pilat (2010a) in the application of 6 pole radial AMB. Our goal is to realise identification tests to determine the actual characteristics of the magnetic field distribution. These studies are necessary to obtain an analytical mathematical model for the synthesis of direct control of the magnetic field, as well research on state estimators. Particular interest is directed towards the observed nonlinearities shown in magnetic field measurements in a rotor-bearing system.

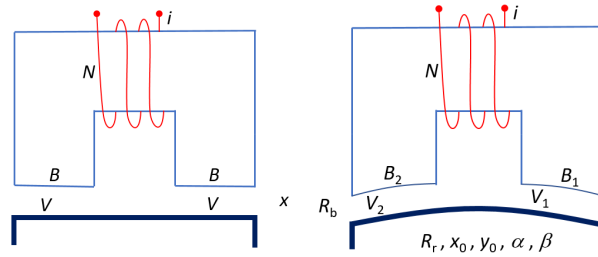


Figure 1: Ideal and real horseshoe in active magnetic bearing.

Typically, an ideal configuration of the C-shaped actuator consisting of  $N$  coil turns and driven by the current  $i$  is considered with a gap volume  $V = 2Ax$ , where  $A$  is a pole area and  $x$  is a rotor displacement. In this case, magnetic flux density is calculated as follows:  $B = 0.5\mu_0 Nix^{-1}$ . In general, the gap volumes  $V_1$  and  $V_2$  vary due to the rotor/bearing radii ( $R_r$ ,  $R_b$ ), and rotor displacement/orientation ( $x_0$ ,  $y_0$ ,  $\alpha$ ,  $\beta$ ). The volume differences are well visible in the case of an elliptic rotor study (see Pilat (2020)). With this research we would like to make a step towards the analytical function describing the magnetic flux density  $B_1$  and  $B_2$  in magnetic bearing poles.

## 2. Radial Active Magnetic Bearing under study

Without a thin-walled magnetic field sensor, the design of the pole piece was prepared to locate a commercially available magnetic field sensor. A dedicated PCB was developed, 8 sensors were mounted, and then embedded into bearing poles. The magnetic bearing characterised by an internal diameter of 51.8mm was not equipped with a safety bearing. Thanks to which, it was possible to identify the relationship of magnetic flux density  $B(\cdot)$  in the full range of 48.5mm diameter rotor displacements and a limited range of currents ( $0 \div 2A$ ).

## 3. Investigation of prototype and digital twin.

Experimental studies were carried out using two actuators located oppositely on the  $Y$  axis: EM1 and EM3. The maximum rotor levitation gap is 3.3mm. Each of them was independently controlled by voltage signals  $U_1$  and  $U_3$ , resulting in current flow with the intensity of  $I_1$  and  $I_3$ , respectively. Thus, measurements of magnetic flux density in each of the pole pieces  $B_{11}$ ,  $B_{12}$  for EM1 and  $B_{31}$ ,  $B_{32}$  for EM3 were obtained, respectively. By linearly controlling the triangular signal with a slope of 2 [V/s], a slight hysteresis was observed in the current signal and changes in magnetic flux density related to the rotor location in terms of the amplitude and width of the hysteresis loop (see Fig. 3a). A step change in the control voltage results in a change in the current that also depends on the location of the rotor, which is then visible in the magnetic flux density measurements (see Fig. 3b). The Bode diagrams obtained by harmonic excitation and parametric optimisation resulted in magnetic flux density to current magnitude  $M_{ij}$  and phase shift  $\phi_{ij}$ . The higher values correspond to the rotor short cut in the magnetic circuit (see Fig. 4). The results of these tests showed the properties of the magnetic circuit and the ability to identify the position of the rotor. Precise identification requires the use of a tool that fixes the rotor in the bearing space.

The device was prototyped using the methodology presented by Pilat (2010b). The numerical model called a digital twin was developed in the COMSOL Multiphysics and reflects the prototype configuration. The stator is

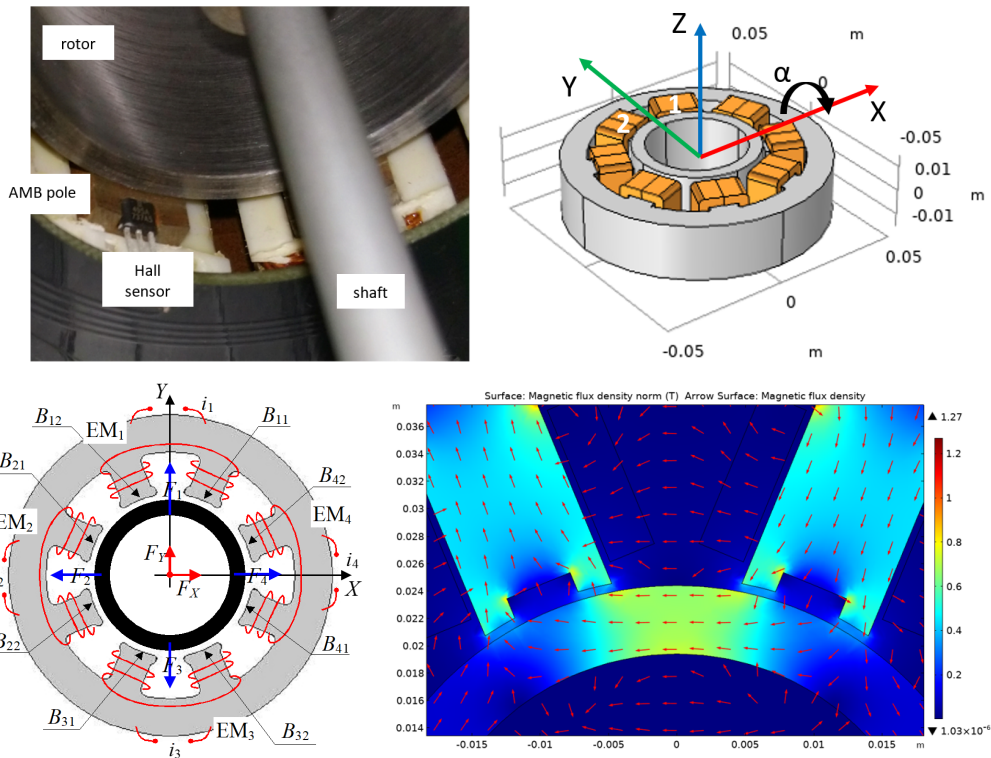


Figure 2: Radial Active Magnetic Bearing prototype with pole embedded magnetic sensors, Digital-Twin of the considered configuration, schematic bearing diagram, magnetic flux density distribution - cross section at the Hall sensor plane.

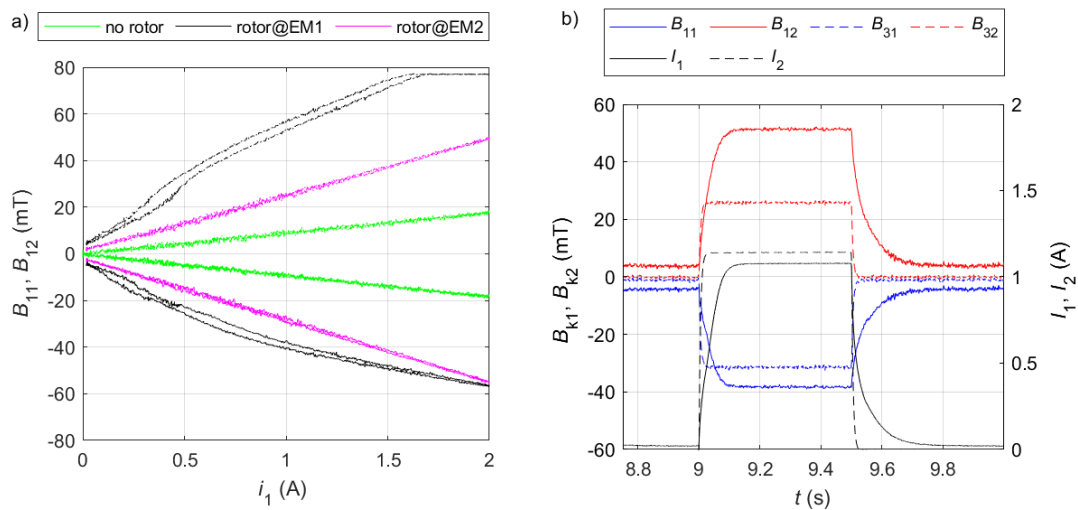


Figure 3: Experimental investigation of magnetic flux density under control: a) triangular excitation, b) square excitation.

modelled as solid, and the coils are modelled as multi-turn with a shape that reflects those produced.

The magnetic flux density measurement points were located in the holes where the Hall sensors are embedded. Using the capabilities of the software, the  $B_X$  and  $B_Y$  components of the magnetic field at the locations of the real sensor were studied and used in calculations. Simulation tests were carried out under stationary

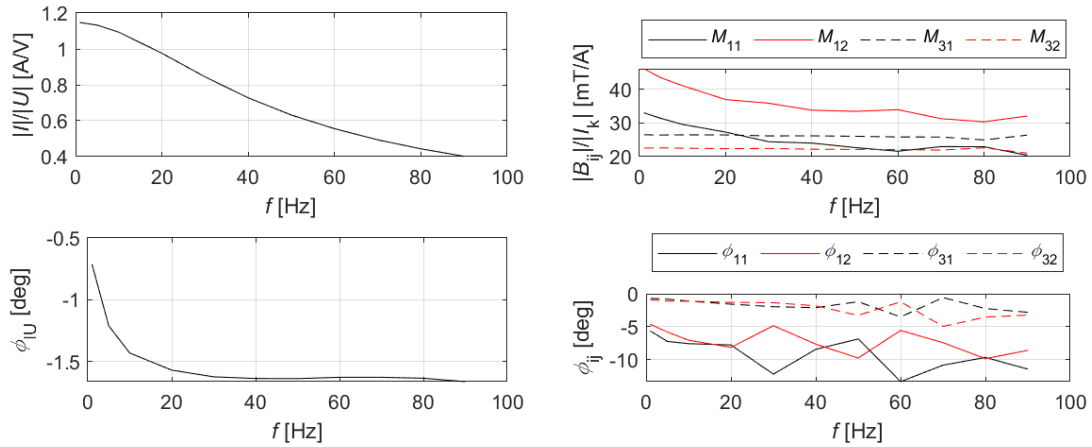


Figure 4: Experimental investigation of magnetic flux density - Bode diagram.

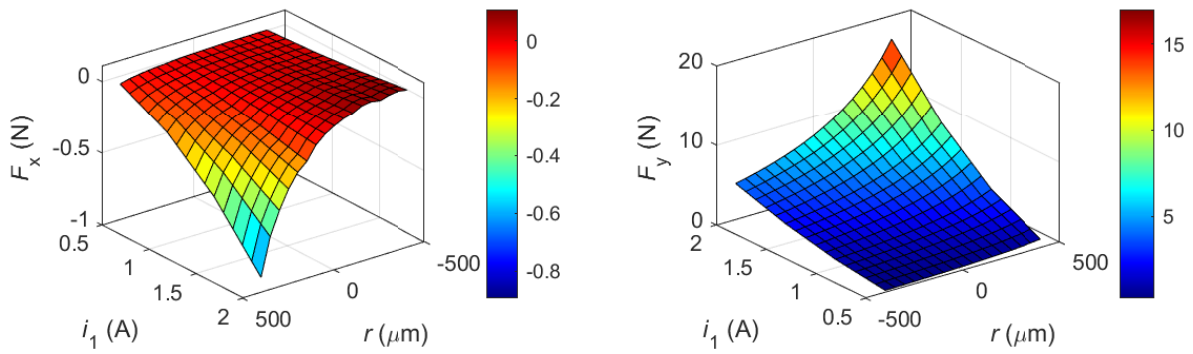


Figure 5: Electromagnetic force components  $F_x$  i  $F_y$  as a function of radial displacement and coil current.

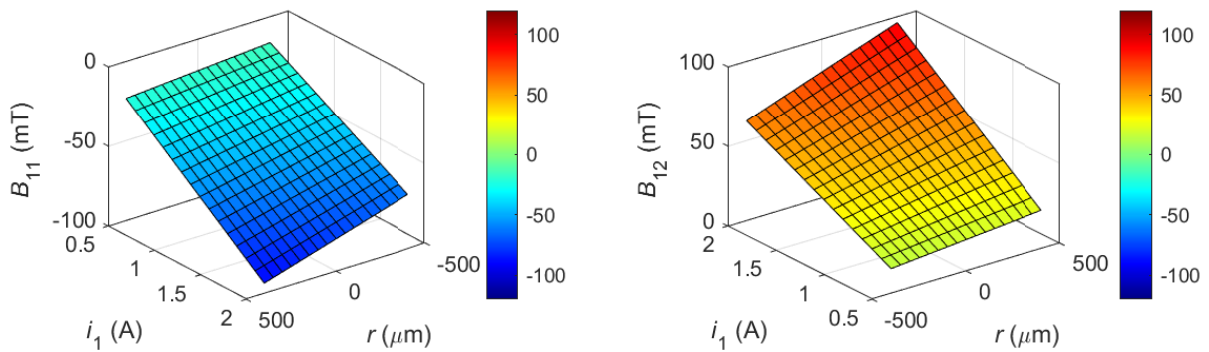


Figure 6: Radial magnetic flux density at AMB poles  $B_{11}(r, I_1)$ ,  $B_{12}(r, I_1)$  as a function of radial displacement and coil current.

conditions assuming a defined value of the current in the coil windings.

The digital twin was diagnosed under different conditions, such as axial motion in the  $X$  and  $Y$  axis, radial motion in the pole axis and rotation with respect to the  $X$  axis. Geometric constraints related to the geometry of the rotor were taken into account when determining the displacement area and changing its orientation. Due to the limited space of the ISMB conference article the results of the radial displacement are only presented. The development of the digital twin made it possible to carry out research, the implementation of which under

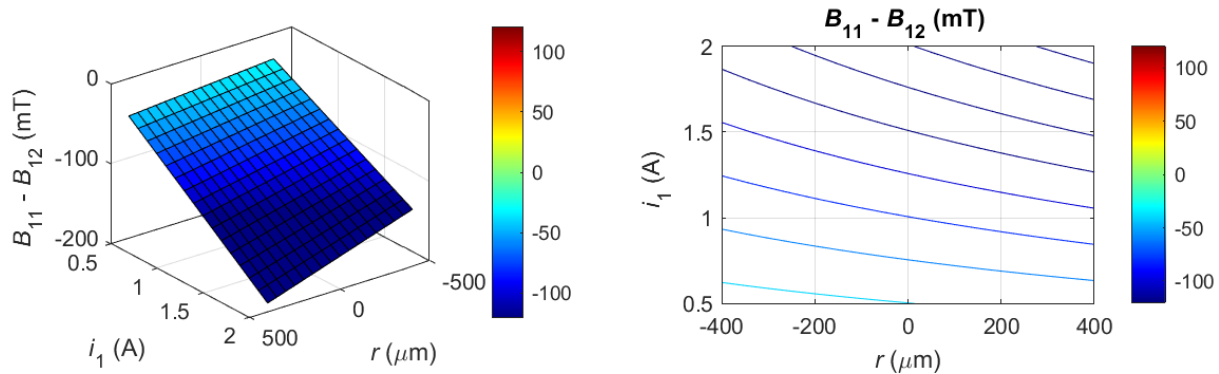


Figure 7: Difference between magnetic flux density measured at both poles  $B_{11}(r, I_1)$ ,  $B_{22}(r, I_1)$  at radial rotor displacement.

experimental conditions is difficult or requires the involvement of specialised equipment. It was subjected to simulation tests to obtain the characteristics of the electromagnetic force  $F(\cdot)$  and the magnetic flux density  $B(\cdot)$  as functions of the current and the position and orientation of the rotor. By moving the rotor along the axis  $Y$  - along the axis of the electromagnet, a symmetrical distribution of the magnetic field in both pole pieces and the known characteristics of the electromagnetic force were observed. By moving the rotor radially along the axis passing through pole piece No. 2, the asymmetry of the magnetic field distribution (Fig. 6) and force interactions (Fig. 5) were examined. The  $F_x$  component assumes negative values as the gap between the rotor and the pole piece decreases. The asymmetry in the measurement of magnetic flux density is clearly visible in this case and assumes a nonlinear character.

Differences between the values of magnetic flux density recorded by virtual sensors placed in the pole pieces were determined, illustrating the nonlinear nature as a function of the rotor position and current (see Fig. 7).

#### 4. Discussion and Conclusions

The idea of embedding Hall sensors in pole pieces turned out to be important from the research and application point of view. The development of such a solution required an analysis of the limitations resulting from the capabilities of the electromagnetic actuator, the measuring range of the sensor and the appropriate mechanical, electrotechnical and electronic design. The developed research configuration allows for carrying out identification tests of the bearing and the rotor in various configurations of the rotating machine. Despite the availability of a single-axis sensor with specific dimensions, which resulted in the preparation of a pole piece structure, the identification of the magnetic field turned out to be effective and showed structural nonlinearity. Placing the sensor in the pole piece requires a trade-off between the measurement range of the sensor and the performance of the actuator. The developed numerical model allowed one to obtain a number of static characteristics illustrating the electromagnetic force and its individual components, as well as the components of the magnetic field vector in each of the slots of the pole piece. This model allowed us to set the position and spatial orientation of the rotor. The development of the 3D model was necessary due to the use of undercuts for the sensors and thus the lack of representativeness of the 2D model. The observed nonlinearities extended knowledge and will play a crucial role in analytical model, the controller and observer design based on the magnetic-field measurements.

In summary, it was observed that the commonly accepted simplifying assumption concerning the determination of the electromagnetic force and magnetic flux density on the basis of identical values of both gaps between the pole pieces and the rotor is possible only in a very small range of rotor displacements and only in the axial direction relative to the electromagnet. For full analysis of nonlinearity, it is required to determine the volume of gaps at the pole pieces as a function of the position and orientation of the rotor. The development of an analytical mathematical model describing the strength and distribution of magnetic flux density in the gap requires

the use of nonlinear functions whose arguments are the position and orientation of the rotor and the value of the current. The development of a control using the measurement of magnetic flux density in the gap requires the use of a nonlinear controller for stabilisation in a wide range of changes in the position and orientation of the rotor. Identification of the position and orientation of the rotor in the levitation area is possible through the use of many magnetic field sensors. Modelling and control using magnetic field measurements requires taking into account the influence of temperature due to the stator to sensor heat transfer. In order to precisely determine the relationship between force and magnetic flux density, the actual volume of the levitation gap between the poles and the rotor should be determined.

## References

- Chowdhury, A. & Sarjaš, A. (2016), 'Finite element modelling of a field-sensed magnetic suspended system for accurate proximity measurement based on a sensor fusion algorithm with unscented kalman filter', *Sensors (Switzerland)* **16**(9).
- Ernst, D., Faghih, M., Liebfried, R., Melzer, M., Karnaushenko, D., Hofmann, W., Schmidt, O. G. & Zerna, T. (2020), 'Packaging of ultrathin flexible magnetic field sensors with polyimide interposer and integration in an active magnetic bearing', *IEEE Transactions on Components, Packaging and Manufacturing Technology* .
- Ernst, Mönch, J. I., Bahr, Hofmann, Schmidt & Zerna (2016), Flexible magnetic field sensors with ultra-thin silicon interposer, in '2016 6th Electronic System-Integration Technology Conference (ESTC)', pp. 1–4.
- Kjølhede, K. & Santos, I. F. (2006), 'Experimental Contribution to High-Precision Characterization of Magnetic Forces in Active Magnetic Bearings', *Journal of Engineering for Gas Turbines and Power* **129**(2), 503–510.  
**URL:** <https://doi.org/10.1115/1.2434345>
- Miguel, L., Molina, C., Galluzzi, R., Bonfitto, A., Tonoli, A. & Amati, N. (2018), 'Magnetic Levitation Control Based on Flux Density and Current Measurement', *MDPI Appl. Sci.* .  
**URL:** [www.mdpi.com/journal/applsci](http://www.mdpi.com/journal/applsci)
- Mystkowski, A., Kierdelewicz, A., Jastrzebski, R. P., Dragašius, E. & Eidukynas, D. (2019), 'Flux measurement and conditioning system for heteropolar active magnetic bearing using kapton-foil hall sensors', *Mechanical Systems and Signal Processing* **115**, 394–404.
- Pilat, A. (2010a), 'Active magnetic bearing and control system for active magnetic bearing', *WO 2011074996*, A2.
- Pilat, A. (2010b), 'Analytical modeling of active magnetic bearing geometry', *Applied Mathematical Modelling* **34**(12), 3805–3816.
- Pilat, A. (2020), '6 pole amb as a drive of elliptic rotor – initial study supported by the virtual prototype', *International Journal of Applied Electromagnetics and Mechanics* **63**(1), 153–170.
- Voigt, A. J., Mandrup-Poulsen, C., Nielsen, K. K. & Santos, I. F. (2017), 'Design and Calibration of a Full Scale Active Magnetic Bearing Based Test Facility for Investigating Rotordynamic Properties of Turbomachinery Seals in Multiphase Flow', *Journal of Engineering for Gas Turbines and Power* **139**(5). 052505.  
**URL:** <https://doi.org/10.1115/1.4035176>
- Voigt, A. J. & Santos, I. (2012), Theoretical and experimental investigation of force estimation errors using active magnetic bearings with embedded hall sensors, in 'Proceedings of ASME Turbo Expo 2012'.